Security constrained optimal power flow in a power system based on energy storage system with high wind penetration

Hossein Ebrahimi[1], Mehdi Abapour[1], Behnam Mohammadi Ivatloo[1], Sajjad Golshannavaz [2, *]

[1] Department of Electrical and Computer Engineering, University of Tabriz, Tabriz, Iran

E-mail addresses: h.ebrahimi@ms.tabrizu.ac.ir (Hossein Ebrahimi); abapour@tabrizu.ac.ir (Mehdi Abapour); bmohammadi@tabrizu.ac.ir (Behnam Mohammadi-Ivatloo)

[2*] Electrical Engineering Department, Urmia University, Urmia, Iran

E-mail address: s.golshannavaz@urmia.ac.ir (Sajjad Golshannavaz)

Tel: +98 443 277 56 60

Abstract

This study is focused on assessing the effect of energy storage system (ESS) presence on security improvement of power systems hosting remarkable renewable energy resources. To this end, ESS presence is suitably included in security-constrained optimal power flow (SCOPF) model; the required technical amendments are hence considered. To launch a realistic model, ramping constraints of thermal units are also taken into account, which, limit the generators from completely responding to power shortfalls. Considering a high penetration level of renewable generations, different scenarios of outages in transmission lines and generators are simulated to measure the line outage distribution factor (LODF) and power transfer distribution factor (PTDF). Also, in order to illustrate the economic impact of wind power generation curtailment and load shedding, two penalty parameters value of wind curtailment (VWC) and value of loss of load (VOLL) are considered in the model. Two test systems, including a PJM 5-bus system and an IEEE 24-bus RTS, are put under numerical studies to assess the possible impact of ESS on security improvement of the investigated systems. The obtained results are discussed in depth.

Keywords: Renewable, uncertainty, security-constrained optimal power flow (SCOPF), energy storage system (ESS), security analysis.

1. Introduction

The soaring energy demand of power systems in different sectors including residential, commercial and industrial, calls the need for further investments in power generation facilities. Meanwhile, the generation-consumption balance should be preserved with required reserve capacity. Beyond the conventional central generations which are mainly thermal units, it is now a common practice to deploy distributed generations (DGs) to enhance the economic operation of power systems, increase the supply reliability [1], reducing power losses, suppressing the pollutant emission and etc. Among these, renewable-based DGs such as wind turbines are recognized to be more environmentally-friendly resources [2]. In this context, most of the governments have catered the utilization of these resources in their power generation portfolio. However, the intrinsic uncertainties of these resources pose significant hurdles in power system operation, mainly in security analysis and perseverance. Contingency analysis (CA) is a common task to assess the security level of the power system and to consider preventive schedules.

SCOPF is a powerful tool for safe operation of power systems, specially, when renewable generators such as wind turbine generators are connected to the system and bringing uncertainty to the system [3]. SCOPF is an OPF problem considering some contingencies like generators and lines outages, which the system should be secured against them. SCOPF is the incorporation of minimum cost and safe operation and security of the system [4]-[5]-[6]. To consider the security indices of a power system, there are some effective tools. One of these tools is calculation of linear sensitivity matrices. Authors of [7] have calculated two kinds of linear sensitivity matrices of control variables (i.e. voltage variations, reactive power generation and line flows). In this paper both OPF and SCOPF solutions are obtained by LP and compered against each other. They express that consideration of security constraints would raise operation costs, but any N-1 contingencies will not affect the system. Linear sensitivity factors including power transfer distribution factor (PTDF), line outage distribution factor (LODF) and outage transfer distribution factor (OTDF) are utilized to express the security constraints in the post-contingency state. Typically, SCOPF includes preventive and corrective types, which, differ from each other. In the Preventive SCOPF (PSCOPF), it is not allowed to reschedule control variables in the post-contingency state, except those with automatic responses associated with contingencies [8]. Moreover, it tries to minimize cost function through only variables of normal case control variables which are feasible for both normal and contingency cases. This is while; consideration of C contingencies makes the problem size to be approximately C+1 time larger than the traditional OPF. the Corrective SCOPF (CSCOPF) considers violation of some contingencies which system can handle them without damaging the devices. The total cost obtained by CSCOPF is often smaller than the one from PSCOPF, but model requires some additional variables and maybe a large number of reschedules for every contingency [9]. As it is explained in [10] a secure system is defined at some levels, but the levels which SCOPF treats the system are as follows; Security level 1 is a system which all loads are supplied, no operating limits are violated and no limit violations occur in the event of a contingency. Security level 2 is the one that all loads are supplied, no operation limits are violated and any violations caused by a contingency can be corrected by appropriate control actions without loss of load. Ideal operation condition for a system happens when security level 1 is observed but from the view point of economics security level 2 is more reasonable.

Evaluating the impact of renewables on power system security is of priority owing to their intrinsic uncertainties. Renewable generations like wind generation pose various uncertainties which call the need for security assessing of power system beside them [11]-[12]. To this end, Authors of [13] considered a power system with high wind penetration and developed a security constrained unit commitment (SCUC) model to assess the impact of battery-ESS (BESS) units on the security of the system. To secure the system against the uncertainties of renewable generations, ESSs are one of the most effective tools. But SCOPF for a system without ESSs needs a large model, which makes its solution time consuming [14]. Now, if the ESS is added to the system the model will be very heavy and too much time is needed to solve the problem [15]. A benders decomposition (BD) corresponding to a mixed integer programming (MIP) is used to solve the SCUC problem in [13]. Authors investigated the impact of (BESSs) presence on the security of systems with high penetration of wind power generations. It is illustrated that the BESSs charge in the off-peak time and discharge during the peak time of the system, so the load curve of the system will be smoothened. Also, the presence of BESS in the system reduces the security cost. The SCUC model suffers from the lack of considering the transmission constraints of the power system. In [16] a model based on the AC-SCOPF is developed, but the AC model’s execution time is so excessive that it can’t be utilized for operational purposes. An enhanced corrective SCOPF model is conducted in [17] to evaluate the impact of distributed BESS units on the security of a power system, but renewables are not considered. Among all security concerned power system problems, it can be seen that contingencies to be studied are excessive, so it is time-consuming to consider them all exactly and comprehensively.

Techniques which are being utilized to reduce the number of noted contingencies are named as contingency filtering (CF) techniques. Authors of [18] proposed an iterative approach to solve the SCOPF problem. The process contains six major stages: (1) load flow, (2) SCOPF, (3) Security Analysis (SA), (4) CF, (5) PSCOPF, (6) NC. The security analysis detects the type of contingencies (overload or voltage collapse), the CF scheme is to identify binding constraints to be used in the problem solution, network compression (NC) is used to reduce the complexity of network model. The algorithm used here optimizes both active/reactive power flows together and treats discrete variables. Authors of [19] proposed an integrated method to rank the contingencies of power system. As it is obvious the impact of ESS presence on the security of the power system with high renewable generation penetration by means of SCOPF is still an interesting work to be done.

In this paper, a multi-period multi-stage MINLP DC-SCOPF model is developed to assess the impact of ESS units on the security of a power system with high wind generation penetration, in a 24-hour time period. A 24-hour load curve and a 24-hour airflow pattern is used to model the load and wind flow changes. In order to reduce the power losses of the transmission system, ESS units are sited at the buses where wind turbines are in there [20]. By this way power curtailments of wind turbines are managed in this job [21]. In this work, the effect of ESS presence on security improvement of power systems hosting remarkable renewable energy resources is being assessed. To do this, ESS presence is suitably included in SCOPF model; the required technical amendments are hence considered. To have a realistic model, ramping constraints of thermal generation units are also taken into account which limit the generators from completely responding to power shortfalls. Considering a high penetration level of renewable generations, different scenarios of outages in transmission lines and generators are simulated to measure the line outage distribution factor (LODF) and power transfer distribution factor (PTDF). Also, in order to illustrate the economic impact of wind power generation curtailment and load shedding, two penalty parameters VWC and VOLL are considered in the model. Furthermore, the charging/discharging efficiencies of ESS units are considered, and to reduce the execution time of the model a CF framework is conducted that selects only the binding contingencies. Finally, to illustrate the utilization performance of transmission lines and risk of operating the system, a performance index (PI) calculation is performed. In this paper, the main contributions could be listed as follows:

- Secure operation of power system with high wind penetration is proposed, and comprehensive evaluations on this task are illustrated;
- Wind generation uncertainties are managed by means of ESS units to ensure the security of the system;
- Security cost of the system which consists of line outage and generation outage prohibition costs and consequently the operation cost is reduced;

- Major reduction in number of contingencies posing to the system and hence improvement of the system security.

2. Model formulation

Mathematical formulation of the SCOPF model in a system coordinated with wind generation and ESS is provided in this section. The model consists of an objective function and its related constraints. The objective function is the operation cost of the system. load flow equation and generation constraints of generators and line flow limits are the constraints of the conventional OPF problem. Security constraints for line outages and generator outages are considered. Also, wind generation constraints are added to the model. Furthermore, the constraints of ESS units' operation, including the state of charge (SOC) of units, maximum charge/discharge for each unit at each time interval and a constraint for asynchronous charge/discharge for each unit, are brought in the model.

2.1. Objective function

The objective function for this problem to be minimized consists of generating units' operation costs and load shedding penalty and the value of wind curtailment at each period.

$$OF = \sum_{g,t} (a_g (P_{g,t})^2 + b_g P_{g,t} + c_g) + \sum_{i,t} (VOLL \times LS_{i,t} + VWC \times P_{i,t}^{wc}) \tag{1}$$

2.2. OPF constraints

The constraints of the conventional OPF problem for generating units and line flow limits, and also, load shedding constraints and wind power generation are as follows.

$$(\sum_{g\in\Omega_G^i} P_{g,t}) + LS_{i,t} + P_{i,t}^w - L_{i,t} - P_{i,t}^c + P_{i,t}^d = \sum_{j\in\Omega_l^i} P_{ij,t} \quad : \lambda_{i,t} \tag{2}$$

$$P_{ij,t} = \frac{\delta_{i,t} - \delta_{j,t}}{x_{ij}} \tag{3}$$

$$-P_{ij}^{\max} \le P_{ij,t} \le P_{ij}^{\max} \tag{4}$$

$$P_g^{\min} \le P_{g,t} \le P_g^{\max} \tag{5}$$

$$P_{g,t} - P_{g,t-1} \le RU_g \tag{6}$$

$$P_{g,t-1} - P_{g,t} \le RD_g \tag{7}$$

$$0 \le LS_{i,t} \le L_{i,t} \tag{8}$$

$$0 \le P_{i,t}^{w} \le w_{i,t} \Lambda_i^{w} \tag{9}$$

$$P_{i,t}^{wc} = w_{i,t} \Lambda_i^{w} - P_{i,t}^{w} \tag{10}$$

Equation (1) is the objective function of the problem. Equation (2) is the load balance equation. Equation (3) explains the power flow equation. Inequality (4) is the thermal constraint of lines. Equations (5), (6) and (7) are thermal generation units' constraints. Equation (8) explains the load shedding constraint. the inequality (9) illustrates the constraint of wind turbines generated active power and Equation (10) illustrates the amount of curtailed active power output of wind turbines.

2.3. Security constraints

The main goal of this paper is to maximize the security of the system. To address the security of the system, security constraints must be added to the model of the power system.

To provide a mathematical base for security considerations, Two security parameters, PTDF and LODF, which are calculated in [22], are used in this article. Also, a parameter to calculate the participation amount of generators when one is out is calculated in [22]. But according to the context of the book, they considered that by increasing the production of each generator according to this parameter, no generator will get to its maximum limit. So, in this paper, the parameter is considered as a variable which takes into account the current generation of generators and then calculates the participation factor.

$$PTDF_{i,j,nm} = \frac{1}{x_{nm}}((X_{ni} - X_{nj}) - (X_{mi} - X_{mj})) \tag{11}$$

$$LODF_{ij,nm} = \frac{X_{in} - X_{im} - X_{jn} + X_{jm}}{x_{ij}\left(1 - \frac{X_{nn} + X_{mm} - 2 \times X_{nm}}{x_{nm}}\right)} \tag{12}$$

$$\gamma_{i,j,t} = \frac{P_{g_j}^{\max} - P_{g_j,t}}{\sum_{\substack{k \\ k \neq i}} (P_{g_k}^{\max} - P_{g_k,t})} \tag{13}$$

$$-1.2 \times P_{ij}^{\max} \leq P_{ij,t} + PTDF_{\mathrm{n},ref,ij} \times P_{n,t}^{g} - \sum_{m \neq n} [PTDF_{ref,\mathrm{m},ij} \times \gamma_{m,n,t} \times P_{n,t}^{g}] \leq 1.2 \times P_{ij}^{\max} \tag{14}$$

$$-1.2 \times P_{ij}^{\max} \leq P_{ij,t} + LODF_{ij,nm} \times P_{nm,t} \leq 1.2 \times P_{ij}^{\max} \tag{15}$$

Equalities (11), (12) and (13) calculate PTDF, LODF and participation factor, respectively. Inequalities (14) and (15) are generation outage and line outage security constraints, respectively. According to [23] the line flow limits for security constraints are considered as short-term emergency limits which are 10-20% greater than normal line flow limits.

2.4. ESS constraints

$$SOC_{i,t} = SOC_{i,t-1} + (P_{i,t}^{c} \eta_c - P_{i,t}^{d} / \eta_d) \Delta t \tag{16}$$

$$U_{i,t}^{c} P_{i,\min}^{c} \leq P_{i,t}^{c} \leq U_{i,t}^{c} P_{i,\max}^{c} \tag{17}$$

$$U_{i,t}^{d} P_{i,\min}^{d} \leq P_{i,t}^{d} \leq U_{i,t}^{d} P_{i,\max}^{d} \tag{18}$$

$$\mathrm{U}_{i,t}^{c} + U_{i,t}^{d} \leq 1 \tag{19}$$

$$SOC_{i,\min} \leq SOC_{i,t} \leq SOC_{i,\max} \tag{20}$$

Constraint (16) illustrates *SOC* content for each ESS unit. Inequalities (17) and (18) are constraints on charge/discharge power for each ESS unit, respectively. Equation (19) is to maintain the asynchronous charge/discharge at ESS units and inequality (20) restricts the amount of *SOC* of each ESS unit.

2.5. Performance index

In order to evaluate the performance of the system before and after the security considerations and also by increasing the load scale, a performance index (*PI*) is introduced in [24] as follows.

$$PI_{MW} = \sum^{\Omega_l} \left(\frac{W_{ij}}{2n} \right) * \left(\frac{P_{ij}}{P_{ij}^{\max}} \right)^{2n} \tag{21}$$

3. Solution method

A three-stage procedure is conducted to solve the SCOPF problem in a system coordinated with wind generation and ESS. (i) In the first stage a conventional OPF is executed to calculate the optimal power flows, bus voltage angles, power outputs of thermal and wind turbine units and the ESS units' charge/discharge amounts. (ii) In the second stage, a CA procedure is performed to take into account only the binding contingencies for the SCOPF problem. In this stage, the power flows calculated in the previous level are being used. (iii) A SCOPF problem considering the binding contingencies acquired in the second stage is administered here.

According to the presence of binary variables related to ESS units' state of charge/discharge, the problem at each stage will be solved as a MINLP problem. A GAMS code is executed for this problem. The SBB solver of GAMS program is utilized to solve the problem in both stages (i) and (iii).

4. Simulation results

In order to evaluate the impact of ESS on the security of the system with high wind penetration, the well-known PJM 5-bus test system and IEEE 24-bus RTS are employed. In order to evaluate the impact of ESS units' presence on the security of the system the total operating cost for the 24-h period from [25] and the number of binding contingencies occurring to the system are compared in 4 scenarios. Scenario 1 doesn't consider both security constraints and ESS units' presence. Scenario 2 only considers the operation of the system with only security consideration. Scenario 3 takes into account the implementation of ESS units but security constraints aren't considered. In scenario 4 both security constraints and employment of ESS units are considered.

4.1. Case study 1: PJM 5-bus test system

The system parameters are as in [26]. As it is shown in Fig. 1, two wind generators and their relative ESS systems are added to buses 1 and 5. The capacity of wind turbine generators at buses 1 and 5 are 125 and 250 MW, respectively. The max. storable energy in the ESS units at buses 1 and 5 are 12.5 and 25 MWh, respectively. The ESS units charging/discharging power at each time interval is $0.2*SOC_i^{max}$, charging efficiency (η_c) for all ESS units is 95% and discharging efficiency (η_d) is 90%. There are two penalty factors in the model. The value of wind curtailment (VWC) is set to 5 $/MW and the value of loss of load (VOLL) is set to 250 $/MW.

Fig. 1. PJM 5-bus test system with wind generations and ESS units

In this system, the total peak demand is 900 MW, the total installed thermal generation capacity is 1530 MW, total installed wind turbine generation is 375 MW and total installed ESS units are 37.5 MWh. Operation cost and number of affecting contingencies of each scenario are illustrated for PJM 5-bus test system in Table 1.

Table. 1. PJM 5-bus test system operation cost and security comparison

As it is obvious the number of binding contingencies is reduced by 63%, and the cost of security from scenario 2 to scenario 4 is reduced by 65.2308 $ for operation in a 24-h period by the employment of ESS units. Security cost in scenario 2 is 94619.908 $ and in scenario 4 is 94566.8956 $.

Fig. 2 and Fig. 3 illustrate the *SOC* (MW) and total charge/discharge power (MW) of ESS units in the 24-h period of operation, respectively. The ESS units will charge when the gradient of load factor is around zero or when wind factor is high, also, they will discharge when the gradient of load factor is high positive or when the wind factor is low. In other words, ESS units will charge at the off-peak times of system demand and will discharge at peak times of system demand, and also each ESS unit will charge when the related wind turbine isn't curtailing and discharges when it is curtailing the generation. It is obvious that ESS 2 is not dispatched. It is because there is no load in the bus which ESS 2 is there and also the cheapest generation unit is at that bus.

Fig. 2. *SOC* of ESS units for PJM 5-bus test system

Fig. 3. Total charge/discharge power of ESS units for PJM 5-bus test system

Here a performance index calculation for PJM 5-bus test system is performed to see how security considerations affect the utilization performance for branches of the system. according to [24] the smaller the PI_{MW} in one scenario the better the performance of system branches utilization and the lower the risk of the system operation in a scenario. Table 2 shows how security considerations can reduce the amount of risk in the operation of the PJM 5-bus test system. In this table the hourly PI_{MW} are brought to compare them against each other.

Table. 2. PJM 5-bus test system PI_{MW} amount for each scenario

As it is obvious, by comparing the PI_{MW} calculated above between scenario 1 and 2 and scenario 3 and 4, consideration of security constraints reduces the amount of PI_{MW}. Concentrating on the scenarios 2 and 4, shows that when ESS units being discharged at hours 11, 14, 23 and 24 the line flows get slightly higher.

4.2. Case study 2: IEEE 24-bus RTS

The IEEE 24-bus RTS system characteristics are as in [27] and 6 wind generations are added to the system as [28] at buses 3,5,7,16,21 and 23. All wind generators have a 70 MW generation capacity. Also, in this paper, 6 ESS units with 7 MWh capacity are added to every bus with wind turbines. The charging/ discharging efficiency of ESS units is 95% and 90%, respectively. WVC and VOLL are as in case 1. The scenarios are illustrated for IEEE 24-bus RTS are illustrated in Table 3.

Table. 3. IEEE 24-bus RTS operation cost and security comparison

The number of binding contingencies is reduced by 87%, and the cost of security from scenario 2 to scenario 4 is reduced by 143.34 $ for operation in a 24-h period by the employment of ESS units. The cost of security in scenario 2 is 37572.6833 $ and in scenario 4 is 37429.3433 $.

Fig. 4 and Fig. 5 illustrate the *SOC* (MW) and charge/discharge power (MW) of ESS units in the 24-h period of operation, respectively. As in PJM 5-bus test system, the ESS units will charge and discharge during the off-peak and peak times, and also when related wind turbine is not curtailing and when it is curtailing the generation, respectively. It is obvious that ESS 5 is not dispatched. It is because there is no load in the bus which ESS 5 is there and also the cheapest generation unit is at that bus.

Fig. 4. *SOC* of ESS units for IEEE 24-bus RTS

Fig. 5. Total charge/discharge power of ESS units for IEEE 24-bus RTS

In both cases there is no wind curtailment and load shedding, because the wind generation cost is zero and wind curtailment has a penalty and also when considering the security constraints lines do not hit their limits. in the case of load shedding, according to sufficient generation in the test systems there is no need for load shedding.

Just like case 1 in this case performance index is brought in Table 4 to show how security considerations can help improve the risk management in a power system.

Table. 4. IEEE 24-bus RTS PI_{MW} amount for each scenario

By comparing the PI_{MW} calculated above between scenario 1 and 2 and scenario 3 and 4, consideration of security constraints reduces the amount of PI_{MW}. As it can be seen in the scenarios 2 and 4, shows that when ESS units being discharged at hours 6-20 the line flows get slightly higher.

4.3. Load scale manipulation

According to the references that test systems are in there, the load scale in base case of PJM 5-bus test system and IEEE 24-bus RTS are near 0.5 and 0.75, respectively. So, in order to better assess the security of the systems, the load scale will be manipulated as follows, and results are illustrated in Tables 5-8 and Figures 6-9.

<u>*PJM 5-bus test system*</u>

Load scale: 0.75

Table. 5. PJM 5-bus test system operation cost and security comparison

Fig. 6. Total charge/discharge power of ESS units for PJM 5-bus test system with 0.75 load scale

Load scale: 0.95

Table. 6. PJM 5-bus test system operation cost and security comparison

If there be no ESS in the system when load scale is more than 0.75 the problem will be infeasible, but presence of the ESS units make the problem feasible despite the large amount of load shedding.

Fig. 7. Total charge/discharge power of ESS units for PJM 5-bus test system with 0.95 load scale

<u>*PJM IEEE 24-bus RTS*</u>

Load scale: 0.8

Table. 7. IEEE 24-bus RTS operation cost and security comparison

Fig. 8. Total charge/discharge power of ESS units for IEEE 24-bus RTS with 0.9 load scale

Load scale: 0.98

Table. 8. IEEE 24-bus RTS operation cost and security comparison

Fig. 9. Total charge/discharge power of ESS units for IEEE 24-bus RTS with 0.98 load scale

In this case study the system can endure 100% load scale with some load shedding, but the problem will not be infeasible.

5. Conclusion

This paper is concentrated on the impact of ESS on the security of the power system with high wind penetration. Presence of ESS changes the problem from NLP to a MINLP problem. According to the results obtained in the simulations presence of ESS in the power system will reduce the security cost by 0.2% in the PJM 5-bus test system at 0.75 load scale and 3.2% in the IEEE 24-bus RTS at 0.98 load scale. Implementation of ESS units also will mitigate the number of critical contingencies by 59% in the PJM 5-bus test system at 0.75 load scale and 93% in the IEEE 24-bus RTS at 0.98 load scale. Furthermore, results illustrate that ESS units will charge during the off-peak times and will discharge in peak times. This method for dispatching the ESS units will reduce the contingencies imposed on the system by wind generation unavailability. Also, by comparing the results from case studies it can be inferred that, the bigger the system the more the impact of ESS presence on security of the system with high renewable generation penetration.

As a future work the problem can be modeled in a decentralized fashion to make the regional system management possible. Also, the uncertainties of the wind generations will be modeled by probabilistic functions.

Nomenclature

Sets and indices

g	Index of thermal generating units
i, j, n, m	Index of network buses
ref	Reference or slack bus
t	Index of time intervals
Ω_G	Set of thermal generating units
Ω^i_G	Set of thermal generating units connected to bus *i*
Ω_l	Set of network branches
Ω^i_l	Set of branches connected to bus *i*

Parameters

$L_{i,t}$	Power demand in bus *i* at time interval *t*
a_g, b_g, c_g	Cost function coefficients of thermal unit *g*
x_{ij}	Reactance of the branch connecting buses *i* and *j*
PTDF	Power transfer distribution factor
LODF	Line outage distribution factor
P_{ij}^{max}	Maximum power flow limit of branch connecting bus *i* to bus *j*
$P_g^{min/max}$	Minimum/maximum capacity of thermal generating unit *g*
RU_g	Maximum ramp up rate of thermal generating unit *g*
RD_g	Maximum ramp down rate of thermal generating unit *g*
VOLL	Value of loss load
VWC	Value of wind curtailment
Λ_i^w	Capacity of wind turbine connected to bus *i*
η_c	Charging efficiency of ESS units
η_d	Discharging efficiency of ESS units
$P^c_{i,min/max}$	Minimum/maximum charging rate of ESS units
$P^d_{i,min/max}$	Minimum/maximum discharging rate of ESS units
$SOC_{i,min/max}$	Minimum/maximum state of charge of ESS units
Δt	Time interval duration
X_{ij}	Element of row i and column j from inverse of network reactance matrix
$w_{i,t}$	Availability of wind turbine connected to bus *i* at time interval *t*
PI_{MW}	Performance index of lines, containing all line flows normalized by their flow limits
W_{ij}	Real non-negative weighting factor to introduce the impact of a line on the performance of the system. Here it is considered equal to 1.

n Exponent of penalty factor

Variables

OF Objective function

$P_{g,t}$ Active power generated by thermal unit *g* at time interval *t*

$LS_{i,t}$ Load shedding in bus *i* at time interval *t*

$P^{w}_{i,t}$ Active power generated by wind turbine connected to bus *i* at time interval *t*

$P^{wc}_{i,t}$ Curtailed active power of wind turbine connected to bus *i* at time interval *t*

$P^{c}_{i,t}$ Charging power of ESS unit in bus *i* at time interval *t*

$P^{d}_{i,t}$ Discharging power of ESS unit in bus *i* at time interval *t*

$P_{ij,t}$ Power flow on branch connecting bus *i* to bus *j* at time interval *t*

$\lambda_{i,t}$ Locational marginal price (LMP) in bus *i* at time interval *t*

$\delta_{i,t}$ Voltage phase angle in bus *i* at time interval *t*

$SOC_{i,t}$ State of charge of ESS unit connected to bus *i* at time interval *t*

$\gamma_{i,j,t}$ Proportion of generation pickup from unit *j* ($j \neq i$) when unit *i* is out at time interval *t*

$U^{c/d}_{i,t}$ Binary variables for asynchronous charge/discharge of ESS.

References

[1] Yazdaninejadi, A., Hamidi, A., Golshannavaz, S., Aminifar, F., and Teimourzadeh, S. "Impact of inverter-based DERs integration on protection, control, operation, and planning of electrical distribution grids," *Electr. J.*, vol. 32, no. 6, pp. 43–56, 2019, doi: 10.1016/j.tej.2019.05.016.

[2] Y. Nejadi, A., Sattarpour, T., and Farsadi, M. "*Simultaneously optimal placement and operation scheduling of besss and dgs in distribution networks in order to minimizing net present value related to power losses*," vol. 16. 2016.

[3] Mohammadi, J., Hug, G., and Kar, S. "Agent-based distributed security constrained optimal power flow," *IEEE Trans. Smart Grid*, vol. 9, no. 2, pp. 1118–1130, 2018, doi: 10.1109/TSG.2016.2577684.

[4] Bhaskar, M. M. "Security Constraint Optimal Power Flow (Scopf) – a Comprehensive Survey," *Trans. Power Syst. , Proterction Distrib.*, vol. 2, no. June, p. 10, 2011, doi: 10.5120/1583-2122.

[5] Alsac, O., and Stott, B. "Optimal load flow with steady-state security," *IEEE Trans. Power Appar. Syst.*, vol. PAS-93, no. 3, pp. 745–751, 1974, doi: 10.1109/TPAS.1974.293972.

[6] Rahmani, S., and Amjady, N. "Improved normalised normal constraint method to solve multi-objective optimal power flow problem," vol. 12, pp. 859–872, 2018, doi: 10.1049/iet-gtd.2017.0289.

[7] Won , J. R., and Choi, K. "Security-Constrained Optimal Power Flow Using First-Order Contingency Sensitivity Matrix," *IFAC Proc. Vol.*, vol. 36, no. 20, pp. 1019–1023, 2003, doi: 10.1016/S1474-6670(17)34608-6.

[8] Capitanescu, F., Glavic, M., Ernst, D., and Wehenkel, L. “Applications of security-constrained optimal power flows,” *Mod. Electr. Power Syst. Symp. MEPS06*, no. September, p. 7, 2006.

[9] Phan, D. T., and Kalagnanam, J. R.“Some Efficient Optimization Methods for Solving the Security-Constrained Optimal Power Flow Problem,” *IEEE Trans. Power Syst.*, vol. 29, no. 2, pp. 863–872, 2014, doi: 10.1109/TPWRS.2013.2283175.

[10] Dias, L. G., and El-Hawary, M. E. “Security-Constrained Opf: Influence Of Fixed Tap Transformer Fed Loads,” *IEEE Trans. Power Syst.*, vol. 6, no. 4, pp. 1366–1372, 1991, doi: 10.1109/59.116977.

[11] Farsadi, M., Sattarpour, T., and Y. Nejadi, A. “Optimal placement and operation of BESS in a distribution network considering the net present value of energy losses cost,” *ELECO 2015 - 9th Int. Conf. Electr. Electron. Eng.*, pp. 434–439, 2016, doi: 10.1109/ELECO.2015.7394582.

[12] Shahidehpour, M., and Fotuhi-friuzabad, M. “Grid modernization for enhancing the resilience , reliability , economics , sustainability , and security of electricity grid in an uncertain environment,” vol. 23, pp. 2862–2873, 2016.

[13] Prasanta, P., Jain, P., Sharma, S., and Bhaker, R. “Security Constrained Unit Commitment in a Power System based on Battery Energy Storage with High Wind Penetration,” *2018 Int. Conf. Power, Instrumentation, Control Comput.*, pp. 1–6, 2018.

[14] Castillo, A., Gayme, D. F.,and Member, S. “Evaluating the Effects of Real Power Losses in Optimal Power Flow,” vol. 5870, no. c, pp. 1–13, 2017, doi: 10.1109/TCNS.2017.2687819.

[15] Jannati, J., Yazdaninejadi, A., and Talavat, V. “Simultaneous planning of renewable/ non-renewable distributed generation units and energy storage systems in distribution networks,” *Trans. Electr. Electron. Mater.*, vol. 18, no. 2, pp. 111–118, 2017, doi: 10.4313/TEEM.2017.18.2.111.

[16] Thomas, J. J., and Grijalva, S. “Flexible security-constrained optimal power flow,” *IEEE Trans. Power Syst.*, vol. 30, no. 3, pp. 1195–1202, 2015, doi: 10.1109/TPWRS.2014.2345753.

[17] Wen, Y., Guo, C., Kirschen, D. S., and Dong, S. “Enhanced security-constrained OPF with distributed battery energy storage,” *IEEE Trans. Power Syst.*, vol. 30, no. 1, pp. 98–108, 2015, doi: 10.1109/TPWRS.2014.2321181.

[18] Platbrood, L., Capitanescu, F., Merckx, C., Crisciu, H., and Wehenkel, L. “A Generic Approach for Solving Nonlinear-Discrete Security-Constrained Optimal Power Flow Problems in Large-Scale Systems,” *IEEE Trans. Power Syst.*, vol. 29, no. 3, pp. 1194–1203, 2014, doi: 10.1109/TPWRS.2013.2289990.

[19] Simab, M., Chatrsimab, S., Yazdi, S., and Simab, A. “Using integrated method to rank the power system contingency,” vol. 24, pp. 1373–1383, 2017.

[20] de Quevedo, P., and Contreras, J. “Optimal Placement of Energy Storage and Wind Power under Uncertainty,” *Energies*, vol. 9, no. 7, 2016, doi: 10.3390/en9070528.

[21] Shim, J. W., Kim, H., and Hur, K. “Incorporating State-of-Charge Balancing into the Control of Energy Storage Systems for Smoothing Renewable Intermittency,” *Energies*, vol. 12, no. 7, 2019, doi: 10.3390/en12071190.

[22] Wood, A. J., Wollenberg, B. F., and Gerald, S. B. *Power Generation, Operation and Control*, Third. 2014.

[23] Biskas, P. N., and Bakirtzis, A. G. “Decentralised security constrained DC-OPF of interconnected power systems,” pp. 747–754, doi: 10.1049/ip-gtd.

[24] Nangrani, S. P. “Power System Security Assessment using Ranking based on Combined MW-Chaotic Performance Index,” 2015.

[25] “Newyork independant system operator.” [Online]. Available: https://www.nyiso.com/.

[26] Acopf, C. W., F. Li, Member, S., Bo, R., and Member, S. “DCOPF-Based LMP Simulation : Algorithm ,”

vol. 22, no. 4, pp. 1475–1485, 2007.

[27] González, M., and Miguel, J. "An Updated Version of the IEEE RTS 24-Bus System for Electricity Market and Power System Operation Studies."

[28] Pessanha, J. F. M. "Impact of Wind Speed Correlations on Probabilistic Power Flow by using the Nataf Transformation," *2018 IEEE Int. Conf. Probabilistic Methods Appl. to Power Syst.*, pp. 1–6, doi: 10.1109/PMAPS.2018.8440221.

List of figure captions

List of table captions

List of figures

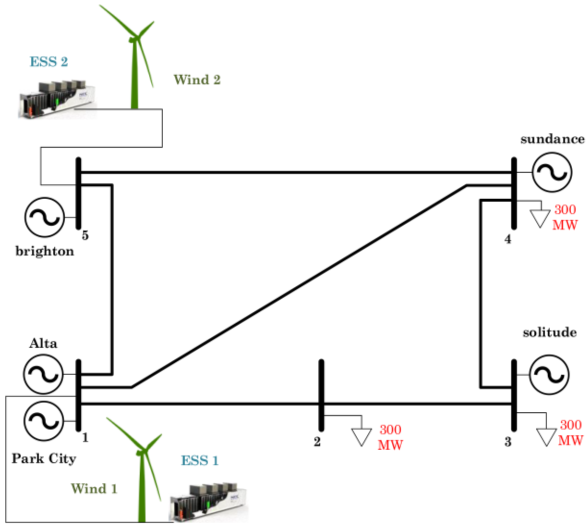

Fig. 1.

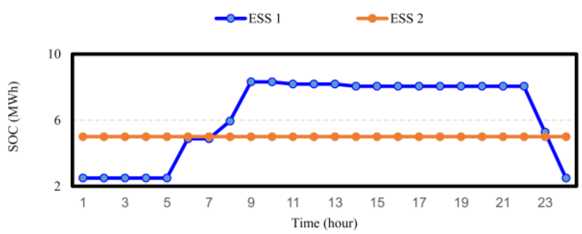

Fig. 2.

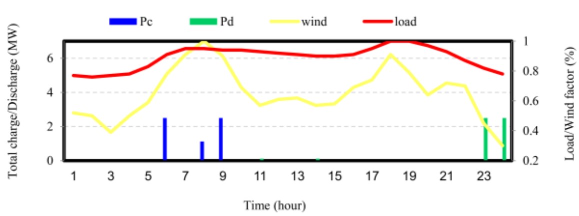

Fig. 3.

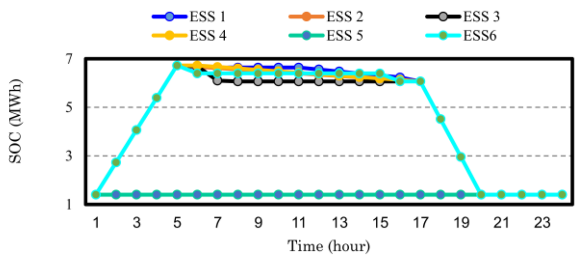

Fig. 4.

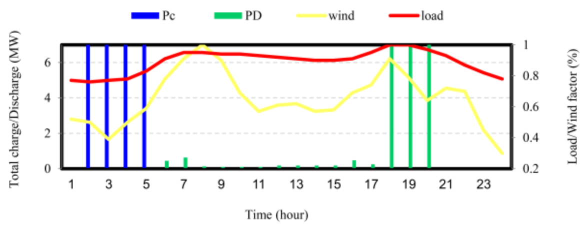

Fig. 5.

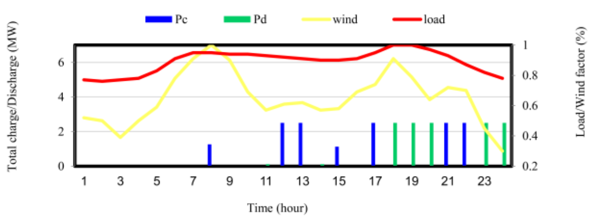

Fig. 6.

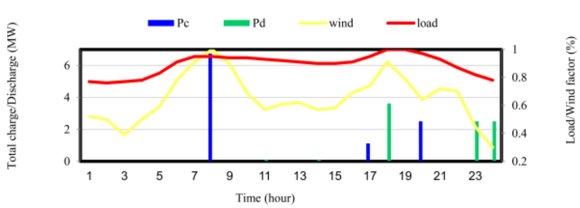

Fig. 7.

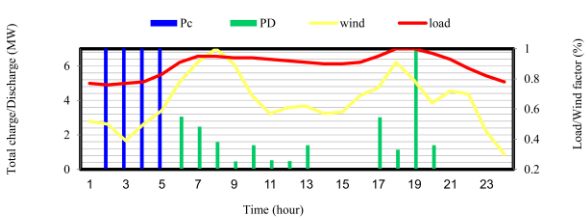

Fig. 8.

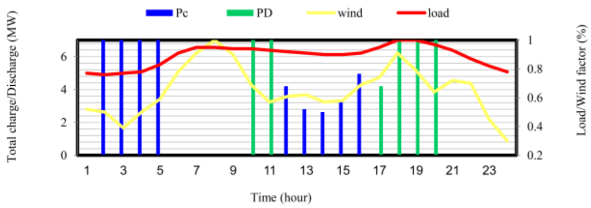

Fig. 9.

List of tables

Table. 1

Scenarios	Operation cost ($)	Number of contingencies
Scenario 1 (no security + no ESS)	175485.4209	-
Scenario 2 (security + no ESS)	270105.3289	667
Scenario 3 (no security + ESS)	175473.2025	-
Scenario 4 (security + ESS)	270040.0981	249

Table. 2

	PI_{MW} (sce.1)	PI_{MW} (sce.2)	PI_{MW} (sce.3)	PI_{MW} (sce.4)
1	0.301506	0.012259	0.301506	0.012259
2	4.448989	0.064956	4.622003	0.064956
3	6.091976	0.052919	6.091976	0.052919
4	4.816728	0.066921	4.816728	0.066921
5	3.413293	0.083014	3.403136	0.083014
6	3.88459	0.094597	3.88459	0.094597
7	4.329712	0.10134	4.329712	0.10134
8	4.362527	0.10134	4.362527	0.10134
9	4.209553	0.099592	4.209553	0.099592
10	4.146316	0.099592	4.146316	0.099592
11	4.016491	0.097715	4.016491	0.097886
12	3.932913	0.096221	3.932913	0.096221

13	3.850276	0.094597	3.850276	0.094597
14	3.764122	0.092848	3.764122	0.093012
15	3.765768	0.093012	3.765768	0.093012
16	3.86451	0.094597	3.868813	0.094597
17	4.272736	0.10134	4.272736	0.10134
18	5.085253	0.110713	5.085253	0.110713
19	5.024076	0.110713	5.024076	0.110713
20	4.493554	0.10496	4.493554	0.10496
21	4.051834	0.097886	4.051834	0.097886
22	3.577483	0.088496	3.577483	0.088496
23	3.378919	0.06463	3.378919	0.067197
24	4.816728	0.044921	4.816728	0.046758

Table. 3

Scenarios	Operation cost ($)	Number of contingencies
Scenario 1 (no security + no ESS)	761361.8655	-
Scenario 2 (security + no ESS)	798934.5488	387
Scenario 3 (no security + ESS)	761336.2647	-
Scenario 4 (security + ESS)	798765.6080	51

Table. 4

	PI_{MW} (sce.1)	PI_{MW} (sce.2)	PI_{MW} (sce.3)	PI_{MW} (sce.4)
1	0.033262	0.012848	0.033262	0.012848
2	0.309456	0.023664	0.303363	0.024184
3	0.264072	0.03081	0.259019	0.031544
4	0.274988	0.031236	0.27122	0.03194
5	0.456938	0.057714	0.448024	0.059023
6	0.506998	0.045753	0.506998	0.045943
7	0.594842	0.038816	0.594842	0.038873
8	0.592553	0.048292	0.592553	0.04834

9	0.568264	0.042405	0.568264	0.042441
10	0.582728	0.028034	0.582728	0.028053
11	0.565786	0.025226	0.565786	0.025242
12	0.530566	0.028566	0.530566	0.028595
13	0.505812	0.031634	0.505812	0.031668
14	0.486932	0.03157	0.486932	0.031604
15	0.486747	0.032191	0.486747	0.032226
16	0.504677	0.036583	0.504677	0.035682
17	0.611476	0.028152	0.611476	0.028187
18	0.678136	0.02533	0.720525	0.026303
19	0.49123	0.020637	0.516026	0.021327
20	0.492093	0.019504	0.517727	0.020232
21	0.549339	0.031461	0.549339	0.031461
22	0.461358	0.068356	0.462951	0.069209
23	0.425005	0.058708	0.42662	0.058708
24	0.28181	0.039617	0.25355	0.039617

Table. 5

Scenarios	Operation cost ($)	Number of contingencies	Total load shedding (MW)
Scenario 1 (no security + no ESS)	482535.0130	-	79.5
Scenario 2 (security + no ESS)	650590.0105	672	349.197
Scenario 3 (no security + ESS)	482535.0130	-	79.5
Scenario 4 (security + ESS)	650254.6309	276	347.957

Table. 6

Scenarios	Operation cost ($)	Number of contingencies	Total load shedding (MW)
Scenario 1 (no security + no ESS)	infeasible	-	-
Scenario 2 (security + no ESS)	infeasible	-	-
Scenario 3 (no security + ESS)	1037233.8768	-	1527.016

Scenario 4 (security + ESS)	2162297.8581	264	5713

Table. 7

Scenarios	Operation cost ($)	Number of contingencies	Total load shedding (MW)
Scenario 1 (no security + no ESS)	811638.7398	-	0
Scenario 2 (security + no ESS)	861851.0572	409	0
Scenario 3 (no security + ESS)	811546.1912	-	0
Scenario 4 (security + ESS)	861711.4492	63	0

Table. 8

Sc enarios	Operation cost ($)	Number of contingencies	Total load shedding (MW)
Scenario 1 (no security + no ESS)	1107265.7058	-	156.719
Scenario 2 (security + no ESS)	1248705.7896	354	505.092
Scenario 3 (no security + ESS)	1107075.2795	-	156.227
Scenario 4 (security + ESS)	1243935.3552	26	405.424

Hossein Ebrahimi received the B.Sc. degree in electrical engineering from Urmia University, Urmia, Iran, in 2013, and the M.Sc. degrees from the electrical engineering from University of Tabriz, Tabriz, Iran in 2019, He is currently pursuing the Ph.D. degree in the School of Electrical Engineering, Urmia University, Urmia, Iran. His research interests include energy management and power system security.

Mehdi Abapour received the BSc and MSc degrees in Electrical Engineering from The University of Tabriz, Tabriz, Iran in 2005 and 2007, respectively, and the PhD degree in Electrical Engineering from The Tarbiat Modares University, Tehran, Iran in 2013. Currently, he is an Assistant Professor at the School of Electrical and Computer Engineering, University of Tabriz. His research interests include reliability, energy management, and power electronics.

Behnam Mohammadi-Ivatloo received the BSc degree in Electrical Engineering from University of Tabriz, Tabriz, Iran in 2006, and the MSc and PhD degrees from Sharif University of Technology, Tehran, Iran in 2008, all with honors. He is currently an Associate Professor at the Faculty of Electrical and Computer Engineering, University of Tabriz, Tabriz, Iran. His main areas of research are economics, operation, and planning of intelligent energy systems in a competitive market environment.

Sajjad Golshannavaz received the B.Sc. (Honors) and M.Sc. (Honors) degrees in electrical engineering from Urmia University, Urmia, Iran, in 2009 and 2011, respectively. He received his Ph.D. degree in electrical power engineering from School of Electrical and Computer Engineering, University of Tehran,

Tehran, Iran, in 2015. Currently, he is an Assistant Professor in Electrical Engineering Department, Urmia University, Urmia, Iran. Since 2014 he has been collaborating with the smart electric grid research laboratory, Department of Industrial Engineering, University of Salerno, Salerno, Italy. His research interests are in smart distribution grid operation and planning studies, design of distribution management system (DMS), demand side management (DSM) concepts and applications, microgrid design and operation studies, design of energy management system (EMS), application of FACTS Controllers in Power systems, application of intelligent controllers in power systems.